ORIGINAL PAPER



Orb weaver glycoprotein is a smart biological material, capable of repeated adhesion cycles

Sean D. Kelly 1 • Brent D. Opell 1 • Lindsey L. Owens 1

Received: 17 August 2018 / Revised: 5 February 2019 / Accepted: 8 February 2019 / Published online: 6 March 2019 © Springer-Verlag GmbH Germany, part of Springer Nature 2019

Abstract

Orb weavers produce webs that trap prey using a capture spiral formed of regularly spaced glue droplets supported by protein fibers. Each droplet consists of an outer aqueous layer and an adhesive, viscoelastic glycoprotein core. Organic and inorganic compounds in the aqueous layer make droplets hygroscopic and cause droplet features to change with environmental humidity. When droplets contact a surface, they adhere and extend as an insect struggles. Thus, a droplet's extensibility is as important for prey capture as its adhesion. Cursory observations show that droplets can adhere, extend, and pull off from a surface several times, a process called cycling. Our study cycled individual droplets of four species—Argiope aurantia, Neoscona crucifera, Verrucosa arenata, and Larinioides cornutus. Droplets were subjected to 40 cycles at two humidities to determine how humidity affected droplet performance. We hypothesized that droplets would continue to perform, but that performance would decrease. Droplet performance was characterized by filament length and force on droplets at pull-off, aqueous volume, and glycoprotein volume. As hypothesized, cycling decreased performance, notably extensibility and aqueous volume. However, humidity did not impact the response to cycling. In a natural context, droplets are not subjected to extensive cycling, but reusability is advantageous for orb-weaving spiders. Moreover, the ability to cycle, combined with their environmental responsiveness, allows us to characterize orb weaver droplets as smart materials for the first time.

Keywords Glycoprotein · Orb weaver · Smart material · Adhesion · Viscous capture droplet · Spider web

Λh	hraviations
AU	breviations

Abbreviat	ions	DT	Droplet thickness
LMMCs	Low molecular mass compounds	GV	Glycoprotein volume
RH	Relative humidity	DV	Droplet volume
L	Length of axial line as hypotenuse	GSA	Glycoprotein surface area
AE	Axial line extension	GR	Glycoprotein ratio
F_{I} /	Force on each axial filament and total force on		

 $F_2/_{total}$ droplet

YMYoung's modulus

 CSA_{AF} Cross-sectional area of axial filament

FLFilament length

Communicated by: Rumyana Jeleva

Electronic supplementary material The online version of this article (https://doi.org/10.1007/s00114-019-1607-z) contains supplementary material, which is available to authorized users

Sean D. Kelly seank6@vt.edu

Department of Biological Sciences, Virginia Tech, Blacksburg, VA 24061, USA

Introduction

Bioadhesives are natural materials that adhere surfaces together and are used by many organisms (Palacio and Bhushan 2012). For example, mussels and barnacles attach to substrates with bioadhesives (Naldrett 1993; Dickinson et al. 2009; Kamino 2010; Waite 2017). Caddis fly larvae and some polychaete annelids use an adhesive to construct a protective tube from sand and shell fragments, and many insects use adhesives to attach their eggs (Mackay and Wiggins 1979; Jensen and Morse 1988; Li et al. 2008). Like most commercial adhesives, these bioadhesives harden after they are applied. In contrast, bioadhesives that are used by sun dews, onychophorans, and orb-weaving spiders remain pliable after they are



produced, ensuring that they spread to establish adhesive contact with insects they capture (Concha et al. 2015; Huang et al. 2015). An orb-weaving spider's adhesive takes the form of regularly spaced viscoelastic glue droplets, which form the capture spiral thread of their web (Fig. 1a). Each droplet consists of a glycoprotein core surrounded by an aqueous outer layer (Fig. 1b). Together, the droplets in a thread span retain an intercepted prey long enough for the spider to locate and subdue it (Blackledge and Eliason 2007). When a series of droplets contact an insect, they extend as the insect struggles, thus combining their adhesive forces and dissipating the energy of the struggling prey (Opell and Hendricks 2007; Sensenig et al. 2013).

Because orb weaver glycoprotein remains pliable, we hypothesize that it functions as a smart material, one that possesses "the ability to change their physical properties in a specific manner in response to specific stimulus input. The stimuli could be pressure, temperature, electric and magnetic

fields, chemicals, hydrostatic pressure or nuclear radiation." (Kamila 2013). Additionally, smart materials must exhibit a reversible behavior or "cycling" in order to be classified as such (Talbot 2003; Smith 2006; Hoogenboom 2014). In the case of our system, orb weaver glue droplets respond to cycling by changing their volume and extensibility as relative humidity changes (Opell et al. 2018a, b). However, the other component of a smart material, cycling, has not been well documented for this bioadhesive. When glycoprotein within droplets that had been flattened on a microscope slide was extended with the tip of a glass probe, the glycoprotein continued to extend for 13 cycles (Sahni et al. 2010). However, the ability of native, suspended droplets to cycle through multiple contact, extension, and pull-off cycles has not been documented. We test our hypothesis by repeatedly adhering individual glue droplets of four orb-weaving species at two different humidities. These individual droplets were adhered to a probe 40 times, and droplet performance was characterized

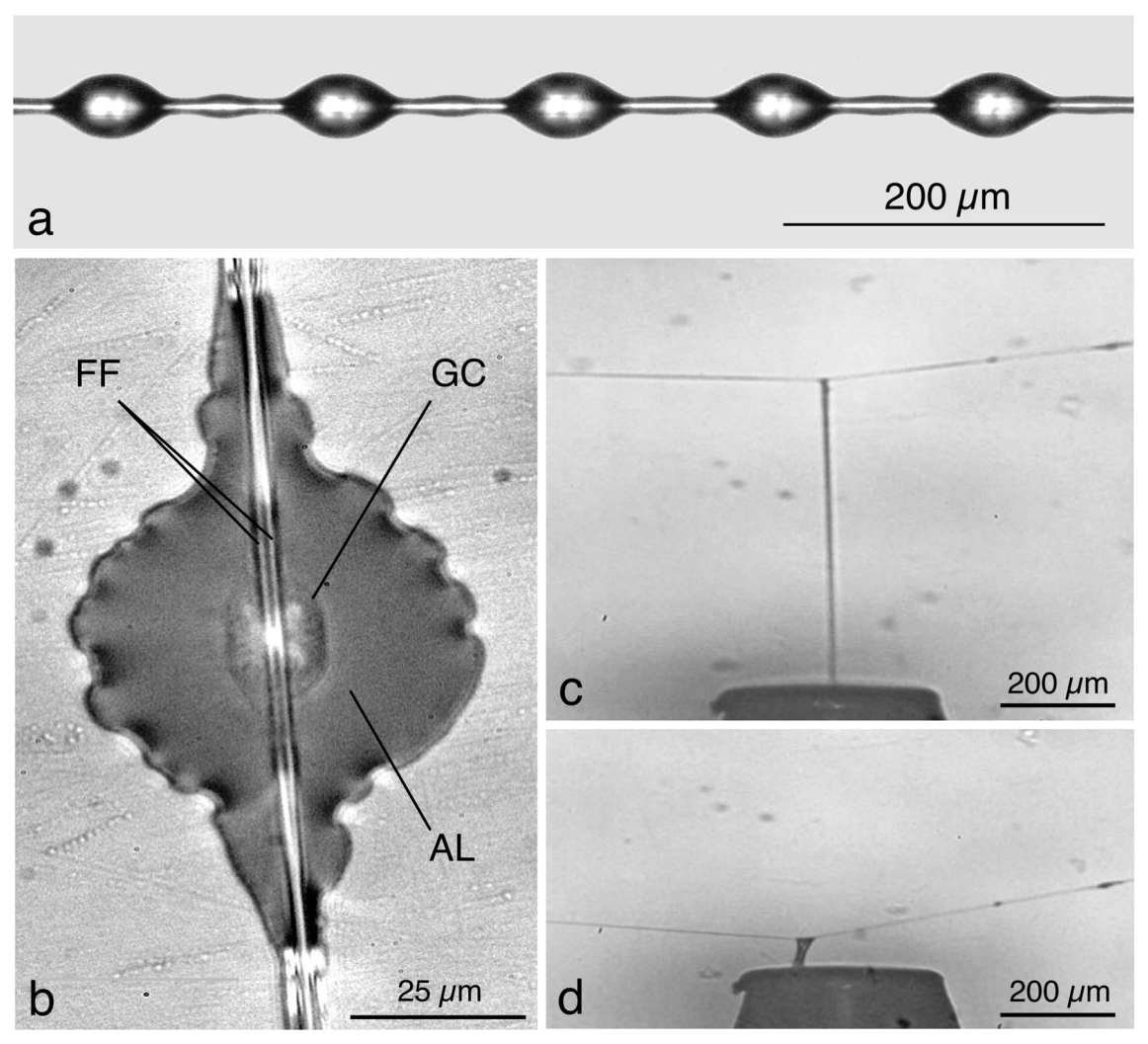


Fig. 1 Argiope aurantia capture thread and droplet features. **a** Capture thread strand with viscous glue droplets. **b** Flattened droplet, showing a pair of flagelliform fibers (FF), glycoprotein core (GC), and aqueous layer

(AL). **c** Extended droplet filament just before pull-off at the first extension. **d** The same droplet at pull-off at fortieth extension



Sci Nat (2019) 106: 10 Page 3 of 15 **10**

throughout adhesion cycles. If cycling is documented, then we can classify orb weaver droplets as smart materials, enhancing their potential for biomimicking studies.

Orb webs are constructed from four types of silk, each secreted by a different gland and exhibiting unique properties (Blackledge and Hayashi 2006; Foelix 2011). The major ampullate glands, situated on the anterior lateral spinnerets, secrete both the stiff frame and radial threads of an orb web (Coddington 1989). Frame threads are attached to surfaces with shock-absorbing pyriform disks and are secreted from a cluster of silk glands of the same name, also located on the anterior spinnerets (Jain et al. 2014; Wolff et al. 2015). Radial threads support the capture spiral and absorb kinetic energy from flying prey (Sensenig et al. 2012). The capture spiral is the product of two types of silk glands, both located on the posterior spinnerets—flagelliform glands, which produce a pair of axial lines, and aggregate glands, which simultaneously cover the axial line in an aqueous glue solution (Edmonds and Vollrath 1992; Opell and Hendricks 2007; Opell et al. 2018a, b). Aggregate glands are unique to the superfamily Araneoidea and are considered to be a key innovation that contributed to the group's evolutionary success (Coddington 1989; Bond and Opell 1998; Blackledge et al. 2009; Townley and Tillinghast 2013). Capture thread is a self-organizing material, whose aqueous layer initially forms a cylinder around the axial threads and then is reconfigured by Plateau–Rayleigh instability into evenly spaced ellipsoid droplets along the supporting axial fibers (Vollrath and Tillinghast 1991; Edmonds and Vollrath 1992; Mead-Hunter et al. 2012). These glue droplets not only trap insects but also play a key role in maintaining the mechanical robustness of the web, with their ability to spool and pack the axial fibers internally, preserving the tension of the capture thread (Elettro et al. 2016).

After a glycoprotein core forms within each droplet, the remaining aggregate gland material remains as an aqueous layer, which covers both the glycoprotein and axial fibers. This layer influences droplet size, as well as glycoprotein adhesion (Vollrath and Tillinghast 1991; Sahni et al. 2014). Low molecular mass compounds (LMMCs) within the aqueous layer, such as choline chloride and N-acetyltaurine, confer hygroscopicity to droplets, causing their volume and performance to change over the course of a day with ambient humidity (Townley et al. 1991; Edmonds and Vollrath 1992). LMMCs also solvate the glycoprotein and improve adhesion, while maintaining the glycoprotein structure (Sahni et al. 2014; Amarpuri et al. 2015a, b). This water plasticizes the capture spiral thread, allowing for greater extension, which is beneficial for prey capture (Vollrath and Edmonds 1989; Blackledge and Hayashi 2006). Natural selection has tuned droplet hygroscopicity by altering the composition of a thread's LMMCs, conferring greater hygroscopicity to threads spun by orb-weaving species that are found in exposed, lower humidity habitats than to the threads of species that occupy humid forest habitats (Opell et al. 2013; Amarpuri et al. 2015a, b).

Although the aqueous layer influences adhesion, the glycoprotein is directly responsible for it, contributing an order of magnitude more adhesion than the capillary force generated by the aqueous layer (Tillinghast et al. 1993; Sahni et al. 2010). At the center of each glycoprotein core, there is a denser region termed a "granule" that appears responsible for anchoring the droplet to the axial lines, minimizing sliding as droplets are extended (Opell and Hendricks 2010). Despite being highly pliable, the glycoprotein is a spidroin (a class of spider scleroproteins) similar to other orb web components (Gatesy et al. 2001; Ayoub et al. 2007; Garb et al. 2010). To date, only one glycoprotein has been characterized—AgSp1 (aggregate spidroin 1) also known as ASG2 (Choresh et al. 2009; Collin et al. 2016). Although glycoprotein is visible only in a droplet's core, proteins are also distributed ubiquitously throughout the aqueous layer (Amarpuri et al. 2015a, b).

When droplets adhere to an insect, the glycoprotein core in each droplet extends, forming an aqueous layer-covered filament that contributes adhesion responsible for holding the insect in place as it attempts to pull free from the web (Fig. 1c). Humidity significantly impacts maximum droplet filament length by altering glycoprotein viscosity (Opell and Sigler 2011; Sahni et al. 2011; Opell et al. 2013; Amarpuri et al. 2015a, b). As mentioned, natural selection has tuned droplet hygroscopicity by altering the LMMC composition, optimizing adhesion in different habitats. This system offers potential for chemists seeking to develop environmentally responsive adhesives. Smart materials are of particular interest for bioinspired development because these materials combine both environmental responsiveness and cycling, the ability to repeatedly perform a task or exhibit a behavior. Examples of such materials include a grass seed's awn, which opens and closes in response to humidity to actively propel the seed into the soil (Elbaum et al. 2007) (Fig. 2).

It is clear that viscous capture droplets are environmentally responsive, although their cycling has not been documented. In nature, a struggling insect is likely to pull free from a thread's glue droplets and, then, re-adhere to them. Thus, there is reason to believe that our cursory observations of droplets re-adhering and extending several times after pull-off are integral characteristic of viscous capture thread performance. In our experimental system, one droplet cycle consists of adhesion to a surface, extension, and pull-off. The objective of this study was to test the following hypotheses: (1) orb weaver glycoprotein is capable of cycling many times with only moderate loss of performance and (2) humidity affects cycling durability, with a more pronounced decrease at low humidity. We characterized droplet cycling by capturing videos of extending droplets and still images of suspended droplets before and after each of 40 cycles. From these, we determined the following: (1) droplet filament length at pull-off, (2) force on a



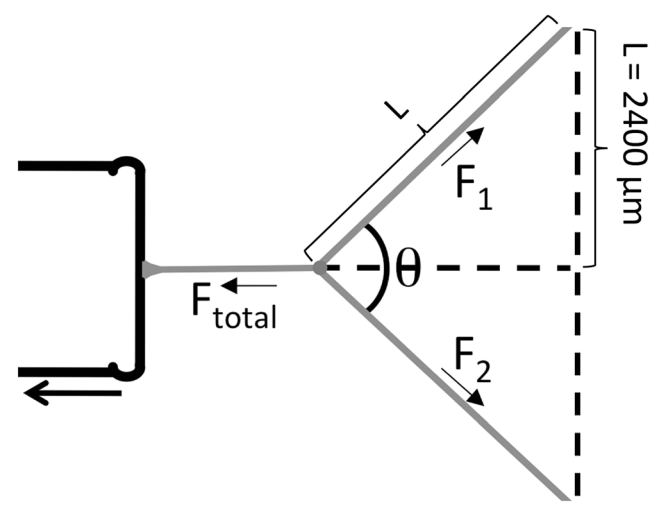


Fig. 2 Diagram visualizing how force on a droplet at pull-off is calculated

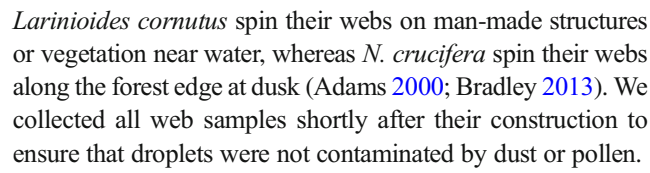
droplet at pull-off, (3) droplet volume and symmetry, and (4) glycoprotein surface area. We tested these hypotheses by characterizing the cycling of four orb-weaving species' droplets. Each species' droplets were cycled at two humidities, representing the upper and lower ranges of humidity encountered during its foraging period.

Changes in glycoprotein performance during cycling would be expressed as a reduction in maximum droplet extension and by less force on an extended droplet at pull-off, as gauged by the deflection of the droplets' support line. Repeated cycling may also affect how LMMCs bind to glycoproteins, an interaction that is crucial for maintaining glycoprotein structure (Amarpuri et al. 2015a, b). This could also indirectly impact glycoprotein viscosity by adding or subtracting LMMCs from the aqueous layer, thereby altering droplet hygroscopicity and volume (Amarpuri et al. 2015a, b).

Materials and methods

Collecting and preparing threads

We collected orb web samples from 9 to 11 mature females of the following species: *Argiope aurantia* (Lucas 1833), *Verrucosa arenata* (Walckenaer 1842), *Larinoides cornutus* (Clerck 1757), and *Neoscona crucifera* (Lucas 1839). We collected these samples from August 1st to September 29th 2017 near Blacksburg, Virginia. *Argiope aurantia* build their webs in exposed weedy habitats before dawn for use throughout the day (Enders 1977). *Argiope aurantia* droplets are very hygroscopic, which is an advantage when relative humidity drops in late morning and afternoon (Opell et al. 2013). *Verrucosa arenata* is diurnal like *A. aurantia*, but its shaded forest habitat exposes its webs to higher humidities than *A. aurantia* (Gaddy 1987; Opell and Hendricks 2009). *Larinoides cornutus* and *N. crucifera* are both nocturnal but vary in their microhabitat.



A 15×52 -cm rectangular aluminum frame with double-sided 3M tape (3M #9086K29550360) on one face was pressed against capture threads in the outer part of a web, securing the contacting threads and separating the sample from the web. After collection, we placed the frame in a closed container for transport to the laboratory, where they were stored at 50-55% relative humidity (RH). We marked the web's position with flagging tape to prevent resampling.

To ensure that we extended only fresh droplets, we completed all extension trials within 17 h after thread collection. We collected individual threads using a pair of forceps with double-sided carbon tape (Cat #77816, Electron Microscope Sciences, Hatfield, PA, USA) wrapped around the tips. These forceps were blocked open to accommodate the supports on a microscope slide sampler where threads were placed. After the forceps tips contacted a thread, we used a hot probe to sever the thread from the web sample. These procedures ensured that threads placed on sampler remained at their native tensions. The microscope slide sampler consisted of four U-shaped brass supports, spaced at 4.8 mm intervals with their upper surfaces covered with carbon tape (Opell and Sigler 2011).

Extending droplets

After collecting the thread samples, we isolated a droplet at the center of the 4.8 mm thread span. To do this, we first sharpened the tip of a small wooden applicator stick so that a few fibers extended and saturated the tip in distilled water. Using this fine point, we slid away the droplets on either side of the focal droplet.

Samplers were placed in a glass-covered observation chamber that rested on the mechanical stage of a Mitutoyo inspection microscope. The chamber maintained a temperature of 23 °C and permitted control of humidity during trials (Opell et al. 2013). We extended individual droplets from each species at two relative humidities separated by 18% RH, chosen to represent divergent, but representative values from each species' habitat. The values were based on measurements of these species' droplet extensions (Opell et al. 2013). We selected lower values (37% and 55% RH) for *A. aurantia* based on its exposed habitat and highly hygroscopic droplets (Enders 1977; Carrel 2008; Opell et al. 2013). We selected higher values (55% and 72% RH) for the remaining species based on the higher humidity of their habitats and the lower hygroscopicity of their droplets (Gaddy 1987; Adams 2000; Bradley 2013).

Before extending a droplet, we cleaned the 413-µm-wide polished tip of a steel probe with 95% ethanol on a Kimwipe®. We, then, inserted the probe through an adjustable



Sci Nat (2019) 106: 10 Page 5 of 15 10

plate on the side of the observation chamber. After we aligned the probe with the droplet, the plate was secured, and the protruding probe was, then, locked in a device that prevented its movement. The observation chamber holding the thread sample was advanced using the microscope stage's X-axis manipulator, bringing the thread into contact with the probe tip and, then, advanced an additional 250 μ m to ensure droplet adhesion. The droplet was, then, immediately extended at 69.5 μ m s⁻¹ by engaging a stepping motor that activated the microscope X-axis manipulator, while a video recorded the droplet's extension at 60 frames per second.

Each droplet extension cycle consisted of droplet adhesion, droplet extension, and droplet pull-off. Thus, we characterized a droplet's ability to adhere and perform by measuring the following: the length of its extending filament, the force on the droplet at pull-off, and the ability of the droplet to remain attached to the axial line. We extended each droplet 40 times, except in a few cases where the droplet pulled free of the thread and remained on the probe's tip. We designated the 1st, 2nd, 4th, 8th, 16th, 24th, 32nd, and 40th extensions as focal extensions, recording videos of these extensions and capturing an image of the droplet before and after each of these extensions. This was done to emphasize earlier extensions, where we presumed that most changes in droplet performance would occur.

Each cycling sequence was conducted as a series, with the time between cycles determined by the short period needed to advance and contact the probe and start the video recording. As the same operator (SDK) performed all extensions, this interval was uniform throughout the study. Thus, droplet recovery period was very similar between cycles and among species. Although, inter-specific differences in glycoprotein viscosity would affect the rate of recovery, we confine our analysis to comparing only intra-specific effects of cycling.

Characterizing droplet volume and symmetry

Droplet volume was determined from images taken before cycling began and after the 40th extension. We used Onde Rulers v1.13.1 screen caliper (Ondesoft Computing, Inc., Beijing, China) to measure droplet length and width (DL and DW, respectively) of suspended droplets. We also measured another droplet, termed a reference droplet, taken from the same web for use in comparison of the glycoprotein volume, as described subsequently. Droplet volume (DV) was computed using the formula presented in Liao et al. (2015) and shown as follows:

$$DV = \frac{2\pi \left(DW\right)^2 \times DL}{15} \tag{1}$$

This formula assumes that droplets are a symmetrical ellipsoid. While this assumption worked for fresh droplets,

excessive cycling often altered the shape of droplets, making them laterally asymmetrical (Fig. 3b). For these droplets, we relied on the penultimate formula reported in the derivation series that produced the formula shown previously.

$$DV = \frac{16 \pi \left(\frac{DW_1}{2}\right) \times \left(\frac{DW_2}{2}\right) \times \left(\frac{DL}{2}\right)}{15} \tag{2}$$

This formula allowed us to distinguish the asymmetrical protrusion of a droplet on either side of the axial line. However, in more complex instances of asymmetry, we modeled droplet volume as the sum of an ellipse, cones, and cylinders (Fig. 4a,b). Instead of squaring droplet width (DW), we measured each side independently, thus accounting for droplet asymmetry. We characterized the symmetry of droplets throughout cycling by measuring the width of the droplet on each side of its flagelliform fiber midline and dividing the shorter of the two by the longer. Thus, a perfectly symmetrical droplet would have a symmetry index of 1 and asymmetrical droplets' smaller values (Table 1).

The aqueous material that covers each droplet's glycoprotein core also continues into inter-droplet regions, where it covers the flagelliform fibers. Therefore, it is possible that this material may flow from the droplet into the inter-droplet regions with cycling. To determine if this occurred, we measured the diameter of the inter-droplet region approximately one droplet diameter away from the edge of a droplet before cycling and after 40 extension cycles. This allowed us to test the hypothesis that repeated cycling drew aqueous material from a droplet and explained any difference in droplet that we might detect between fresh and cycled droplets (Table 2).

Characterizing visible glycoprotein using reference droplets

After the 40th extension, a droplet was flattened to reveal its glycoprotein core (Fig. 3c,d). We accomplished this by using a magnetically tipped device to drop a 22-mm-diameter coverslip on the threads. Once dropped, we pressed the coverslip against the sampler supports using the steel probe to ensure uniform droplet flattening. We also flattened an unextended reference droplet from the same individual's web, to allow a comparison of the effect of droplet cycling on glycoprotein volume and a droplet's glycoprotein volume to aqueous layer volume ratio.

We determined glycoprotein volume (GV) from droplet thickness (DT) and glycoprotein surface area (GSA). First, we used droplet volume (DV) and flattened droplet surface



10 Page 6 of 15 Sci Nat (2019) 106: 10

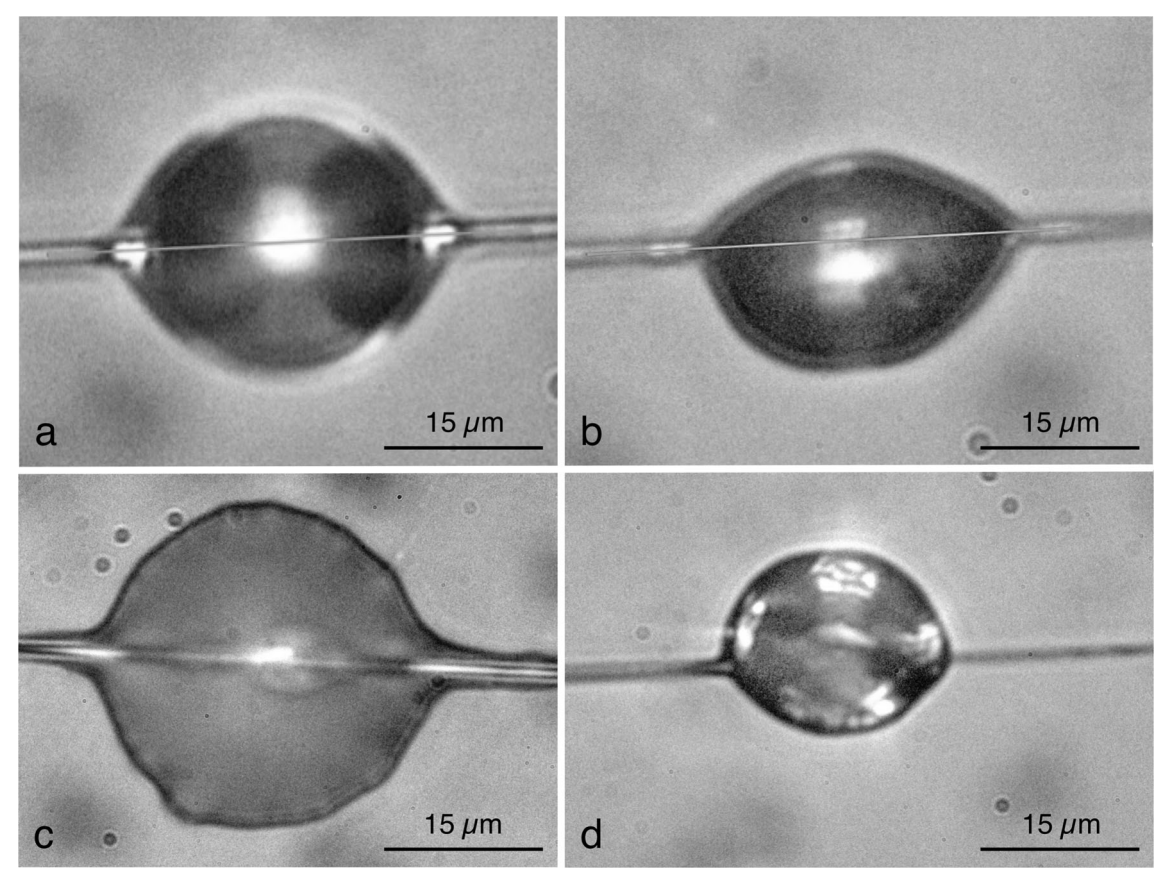


Fig. 3 The effect of cycling on droplet volume, symmetry, and glycoprotein surface area. **a** A suspended *V. arenata* droplet before cycling. **b** The same droplet after 40 extension cycles, noticeably asymmetrical. **c** A flattened *V. arenata* reference droplet. **d** The same droplet after 40 extension cycles

area (DSA) to obtain droplet thickness. The product of DT and GSA gave us GV:

$$DT = \frac{DV}{DSA} \tag{3}$$

$$GV = DT \times GSA$$
 (4)

Glycoprotein ratio (GR) was determined from glycoprotein volume and droplet volume (GV and DV, respectively), using the following formula:

$$GR = GV/DV (5)$$

Characterizing filament length, force on a droplet at pull-off, and estimated work of droplet extension

The length of an extending droplet filament at pull-off was measured using Onde Rulers v1.13.1 screen caliper (Ondesoft Computing, Inc., Beijing, China) (Fig. 1c). Using the method from Opell et al. (2018a, b), we computed the force on droplets at pull-off in four steps (Fig. 2). This approach uses the extension of the paired axial support lines on each side of a droplet with the reported diameters and Young's modulus of these lines (Sensenig et al. 2010) to determine the force on

each side of the deflected support line. These force vectors are, then, resolved to determine the force on an extended droplet filament.

Step 1: Length of the axial line on each side of the extended droplet, computed as a hypotenuse of the right triangle (L) with an opposite side of 2400 μ m and an angle between the hypotenuse and adjacent sides of a right triangle, which is equal to one half of the support line deflection angle (Θ).

$$L = \frac{2400\,\mu\text{m}}{\sin\frac{\Theta}{2}}\tag{6}$$

Step 2: Axial line extension (AE) ratio.

$$AE = \frac{(L - 2400 \mu m)}{2400 \mu m} \tag{7}$$

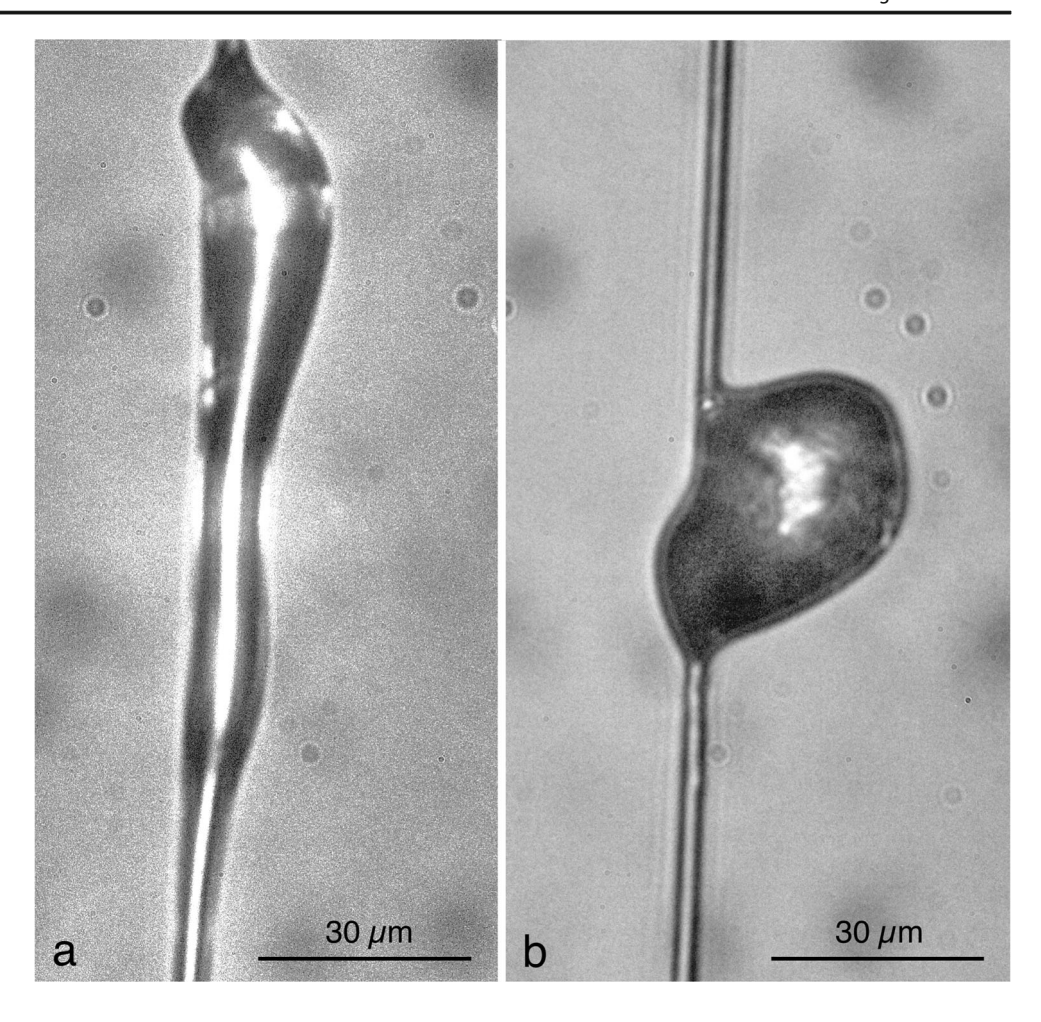
Step 3: Force on axial line (F_1) as a product of Young's modulus (YM), the sum of the two axial line's cross-sectional areas (CSA_{AF}) , and axial line extension (AE). A. aurantia, V. arenata, L. cornutus, and N. crucifera YM = 0.009, 0.098, 0.011, and 0.010 GPa, respectively, and each axial line diameter = 4.8, 1.5, 2.6, and 3.0 μ m, respectively.

$$F_1 = F_2 = YM \times CSA_{AF} \times AE \tag{8}$$



Sci Nat (2019) 106: 10 Page 7 of 15 10

Fig. 4 Two highly deformed *Neoscona crucifera* droplets after cycling. Droplets such as these were rare but required volumes to be determined as a combination of cylinders and cones



Step 4: Force on extended droplet filament (F_{total}) as the resolved force vectors of the two sides of the support line (F_1) , which are equal, using the deflection angle of the support line (Θ) .

$$F_{\text{total}} = 2 \times F_1 \times \sin\left(90^{\circ} - \left(\frac{\Theta}{2}\right)\right) \tag{9}$$

We estimated the work required to extend droplets to pullof as the product of the amount of glycoprotein (glycoprotein volume = GV), its viscosity (droplet thickness = glycoprotein thickness = DT), and the length of its extension (filament length = FL), using the following formula. As this is an estimate, we do not assign units to these values.

Estimated work =
$$FL \times DT \times GV$$
 (10)

Assessing residue on the probe tip after droplet cycling

To determine if repeated cycling left LMMCs or glycoprotein residues on the probe's steel surface, we cleaned a small broken piece of a razor blade with 100% ethanol and contacted it 40 times at 50% RH with an *L. cornutus* droplet. This sample was attached to a scanning electron microscope stub and stored in a desiccator for approximately two weeks, sputter coated with 3 nm of iridium before examination with a LEO (Zeiss) 1550 FESEM (field emission scanning electron microscopy) at the Nanoscale Characterization and Fabrication Laboratory (NCFL) at Virginia Tech, in an attempt to identify compounds in any residue present on the sample.

Analysis

Data were analyzed using SAS JMP (SAS Institute Inc. 1989–2007). We evaluated parameter normality using a Shapiro–Wilk test, considering values with $P \ge 0.05$ to be normally distributed. Parametric and nonparametric tests with $P \le 0.05$ were considered significant. Matched pairs were used for most before–after cycling comparisons.

Four trials were excluded because their droplets pulled off of the axial thread and adhered to the probe. This occurred in one *N. crucifera* individual at 72% RH, one *A. aurantia* individual at 55% RH, and two *V. arenata* individuals at 72% RH.



10 Page 8 of 15 Sci Nat (2019) 106: 10

Table 1 This table shows the most consistent and pronounced changes after cycling. We compare the filament lengths of the first and fortieth cycles as well as droplet volume and the symmetry index before and after cycling. Parentheses indicate sample size and bold P values are considered significant (P<0.05)

Species	Values	Mean filament length (μm)		Mean droplet volume (μm^3)		Mean symmetry index	
		Low RH	High RH	Low RH	High RH	Low RH	High RH
Argiope aurantia ($N = 10$)	Ext 1	1617	1831	43,612	51,358	0.98	0.98
	Ext 40	649	2480	33,441	35,839	0.59	0.74
	SE diff. (±)	215	913	1908	3361	0.07	0.05
	P value	0.0020	0.4956	0.0005	0.0013	0.0003	0.0009
$Verrucosa\ arenata\ (N=10)$	Ext 1	537	779	10,021	12,138	0.96	0.96
	Ext 40	180	186	9115	9070	0.68	0.68
	SE diff. (±)	86	130	986	1136	0.05	0.07
	P value	0.0024	0.0039	0.3820	0.0356	0.0004	0.0058
Larinioides cornutus $(N=9)$	Ext 1	194	315	6245	8000	0.99	0.94
	Ext 40	100	184	5108	5834	0.64	0.67
	SE diff. (±)	27	35	474	523	0.04	0.07
	P value	0.0079	0.0072	0.0433	0.0032	0.001	0.0026
Neoscona crucifera (N = 11)	Ext 1	236	362	21,279	12,661	0.94	0.96
	Ext 40	210	200	15,057	8850	0.60	0.67
	SE diff. (±)	60	147	3154	1089	0.08	0.08
	P value	0.6709	0.3207	0.0891	0.0173	0.0047	0.0195

For these trials, we included only extensions prior to droplet detachment. Droplets that extended fewer than 40 times were included, although this only occurred in two *N. crucifera*

individuals and a single *V. arenata*. One *N. crucifera* individual whose droplet divided into two smaller droplets was excluded from further extensions at low humidity.

Table 2 This table compares the droplet performance at the initial cycle versus the final cycle in terms of the force required to extend a droplet and the estimated work required to do so. Parentheses indicate sample size and bold P values are considered significant (P < 0.05)

Species	Values	Estimated work		Force (µN)		
		Low humidity	High humidity	Low humidity	High humidity	
Argiope aurantia $(N=10)$	1st	7.22×10^{7}	4.47 × 10 ⁷	6.175	1.135	
	40th	3.01×10^{7}	1.69×10^{8}	24.36	6.747	
	Std err (±)	1.75e + 7	8.16×10^{7}	12.084	4.208	
	P value	0.0427	0.1659	0.1806	0.2151	
Verrucosa arenata $(N=10)$	1st	1.99×10^{6}	5.20×10^{6}	6.864	27.322	
	40th	1.38×10^{6}	1.12×10^{6}	4.507	16.507	
	Std err (±)	7.92×10^5	3.30×10^{6}	5.644	6.788	
	P value	0.4613	0.2707	0.6861	0.0983	
Larinioides cornutus $(N=9)$	1st	4.85×10^5	4.87×10^{5}	4.893	8.287	
	40th	2.15×10^{5}	4.57×10^5	3.881	10.386	
	Std err (±)	1.35×10^{5}	1.55×10^{5}	1.136	2.142	
	P value	0.0805	0.8538	0.3990	0.3559	
Neoscona crucifera ($N = 11$)	1st	1.91×10^{7}	2.89×10^{6}	17.943	27.399	
	40th	1.47×10^{7}	7.00×10^{6}	11.887	29.94	
	Std err (±)	8.57×10^{6}	3.14×10^{6}	3.083	4.567	
	P value	0.6248	0.2481	0.0380	0.7232	



Sci Nat (2019) 106: 10 Page 9 of 15 10

Results

Droplet symmetry, droplet volume, and glycoprotein volumes

Droplet symmetry decreased after cycling in all treatments (Table 1). The initial volume of the extended droplets did not differ from that of the reference droplets (Table 3). However, droplet volume decreased in all treatments after cycling except *V. arenata* and *N. crucifera* at low humidity (Table 1, Tables S1–S4). In contrast, glycoprotein volume either remained unchanged or increased (only in *A. aurantia* at 55% humidity) (Table 4). Therefore, as confirmed by the ratio of glycoprotein volume to total droplet volume (Table 4), the decrease in droplet volume resulting from cycling is explained by the loss of aqueous material.

The diameters of inter-droplet diameters were not affected by cycling (P = 0.9096, 0.6741, 0.6029, and 0.2850 for *A. aurantia*, *V. arenata*, *L. cornutus*, and *N. crucifera*, respectively). *Verrucosa arenata* values were compared with a *t* test, whereas the other species were compared with Wilcoxon tests, because one or more values were not normally distributed. Therefore, the hypothesis that repeated cycling drew aqueous material from a droplet was refuted, and any change in droplet volume must be explained by another mechanism.

Droplet extension length

Mean filament length at pull-off shortens after 40 cycles in most treatments (Table 1, Tables S1–S4). This occurs at both

rere not normally distributed. Expected cycling drew aqueous ted, and any change in droplet nother mechanism.

The effect of hu

To determine if h length as a result crease in filament ities of each speci filament length aft P > 0.2207 for ASpecies

Values

Comparis

Table 3 "Fresh" droplets are cycled droplets before their trials, and reference droplets are droplets from the same web that allow for a comparison of glycoprotein characters. In all cases but one, the mean volumes between droplets of the same web did not differ. Parentheses indicate sample size and bold P values are considered significant (P < 0.05)

Species	Values	Comparisons of mean reference and fresh volumes (μm^3)			
		Low RH	High RH		
Argiope aurantia ($N = 10$)	Reference	42,424	48,674		
	Fresh	43,612	51,358		
	SE diff. (±)	2929	2424		
	P value	0.6946	0.2969		
Verrucosa arenata (N = 10)	Reference	9612	11,036		
	Fresh	10,021	10,993		
	SE diff. (±)	824	576		
	P value	0.6317	0.9412		
Larinioides cornutus (N = 9)	Reference	6514	5431		
	Fresh	6245	8000		
	SE diff. (±)	1074	701		
	P value	0.8086	0.0063		
Neoscona crucifera ($N = 11$)	Reference	15,677	12,768		
	Fresh	19,728	14,612		
	SE diff. (±)	2438	1867		
	P value	0.1352	0.3523		

in *A. aurantia*. However, cycling did not decrease filament length for *A. aurantia* at high humidity or *N. crucifera* at either humidity. To create an index of droplet extension length that was not affected by the variability in the length of focal extension 1, we determined the deviation of each individual's droplet length at pull-off from the mean lengths of the eight focal extensions. These values typically decreased during cycling (Figs. 5 and 6). However, in *N. crucifera*, at low humidity, there was no change in filament length, and, in *A. aurantia*, at high humidity, filament length appeared to increase (Figs. 5d and 6a).

humidities in V. arenata and L. cornutus and at low humidity

Force on droplet at pull-off and estimated work

Force on a droplet at pull-off only decreased after cycling in *N. crucifera* at low humidity, while it was unaffected in the remaining 7 treatments (Table 2). The estimated work required to extend the droplet to pull-off after cycling decreased in *A. aurantia* at low humidity, but not in other treatments (Table 2).

The effect of humidity on extension cycling

To determine if humidity affected the decline in filament length as a result of cycling, we compared the percent decrease in filament length after cycling at high and low humidities of each species. Humidity did not affect the decline in filament length after cycling for any of the species (Wilcoxon P > 0.2207 for A. aurantia, $Larinioides\ cornutus$, and



10 Page 10 of 15 Sci Nat (2019) 106: 10

Table 4 Using reference droplets, we were able to compare glycoprotein characters between cycled and uncycled droplets. Glycoprotein ratio = glycoprotein volume / droplet volume. The increase

in glycoprotein ratio after cycling indicates a decrease in aqueous layer volume. Parentheses indicate sample size and bold P values are considered significant (P < 0.05)

Species	Values	Thickness	(μm)	Glycoprotein volume (μm³)		Glycoprotein SA (μm ³)		Glycoprotein ratio	
		Low RH	High RH	Low RH	High RH	Low RH	High RH	Low RH	High RH
Argiope aurantia $(N=10)$	Reference	5.536	4.536	7033	5431	1249	1198	0.15	0.11
	Cycled	5.467	4.779	8715	9805	1516	2044	0.25	0.26
	SE diff.	0.401	0.200	1153	1432	115	304	0.033	0.042
	P value	0.4760	0.3180	0.1826	0.0157	0.0447	0.0237	0.0126	0.0066
$Verrucosa\ arenata\ (N=10)$	Reference	3.003	3.031	1471	1141	550	368	0.16	0.09
	Cycled	3.213	3.489	2129	1892	665	591	0.26	0.27
	SE diff.	0.191	0.875	474	336	164	116	0.034	0.045
	P value	0.3004	0.8257	0.1984	0.0756	0.5017	0.0965	0.0161	0.0052
Larinioides cornutus $(N=9)$	Reference	3.438	2.072	682	483	196	228	0.11	0.08
	Cycled	4.131	2.819	601	768	171	299	0.11	0.13
	SE diff.	1.022	0.225	140	134	27	44	0.013	0.010
	P value	0.5165	0.0105	0.5791	0.0664	0.3720	0.1477	0.8794	0.0018
Neoscona crucifera ($N = 11$)	Reference	9.641	4.286	3957	2513	323	679	0.19	0.26
	Cycled	9.459	9.5	5025	3188	491	399	0.35	0.37
	SE diff.	1.950	1.257	1562	735	76	317	0.050	0.080
	P value	0.5849	0.1689	0.5165	0.4006	0.0573	0.4102	0.0122	0.2368

Neoscona crucifera; t test P = 0.3830 for V. arenata). Thus, the hypothesis that humidity affects the performance of glycoprotein during cycling was not supported by droplet filament length.

Examination of droplet residue

FESEM examination revealed what we interpret to be several concentric rings of LMMC deposits and two small glycoprotein deposits following 40 droplet extensions (Fig. 7). However, these deposits were not thick enough to allow elemental analyses.

Discussion

Impact of cycling on droplet properties and performance

Previous studies have shown that viscous capture threads respond to changes in environmental humidity (Opell et al. 2018a, b). The current study's results support the hypothesis that orb weaver capture spiral droplets are capable of extensive cycling, a performance characteristic that is widely associated with a smart material (Hebda and White 1995; Talbot 2003; Smith 2006). However, the hypothesized greater decrease in droplet performance at low humidity was not supported. Many droplet characteristics did not change in

response to cycling, showing that capture droplets are still functional after extensive reuse. The most pronounced and consistent change associated with cycling was a reduction in filament length at pull-off.

Glycoprotein surface area remained unchanged or, in *A. aurantia*, increased at both humidities. The force on a droplet filament at pull-off remained unchanged in all but *N. crucifera* at low humidity. Taken together, these observations indicate that cycling increases the cohesion of a droplet's glycoprotein, such that pull-off force is reached at shorter filament length. Another expression of this increased glycoprotein cohesion is the ability of a droplet to return to its initial symmetrical, ellipsoid configuration. After extensive cycling, many droplets became asymmetrical and did not regain their original shape (Fig. 4), indicating that their glycoprotein cores were stiffer.

Another notable effect of cycling was the decrease in droplet volume. Measurements of inter-droplet diameter do not support the flow of aqueous material out of the droplet and require another explanation. The presence of suspected LMMCs and glycoprotein residues on a surface after 40 droplet cycles suggests another mechanism. Comparison of glycoprotein volume before and after cycling does not suggest that glycoprotein loss accounts for a reduction in filament length. However, the presence of putative LMMC deposits could explain the reduction in a droplet's aqueous volume after cycling as well as an increase in glycoprotein cohesion, because LMMCs



Sci Nat (2019) 106: 10 Page 11 of 15 10

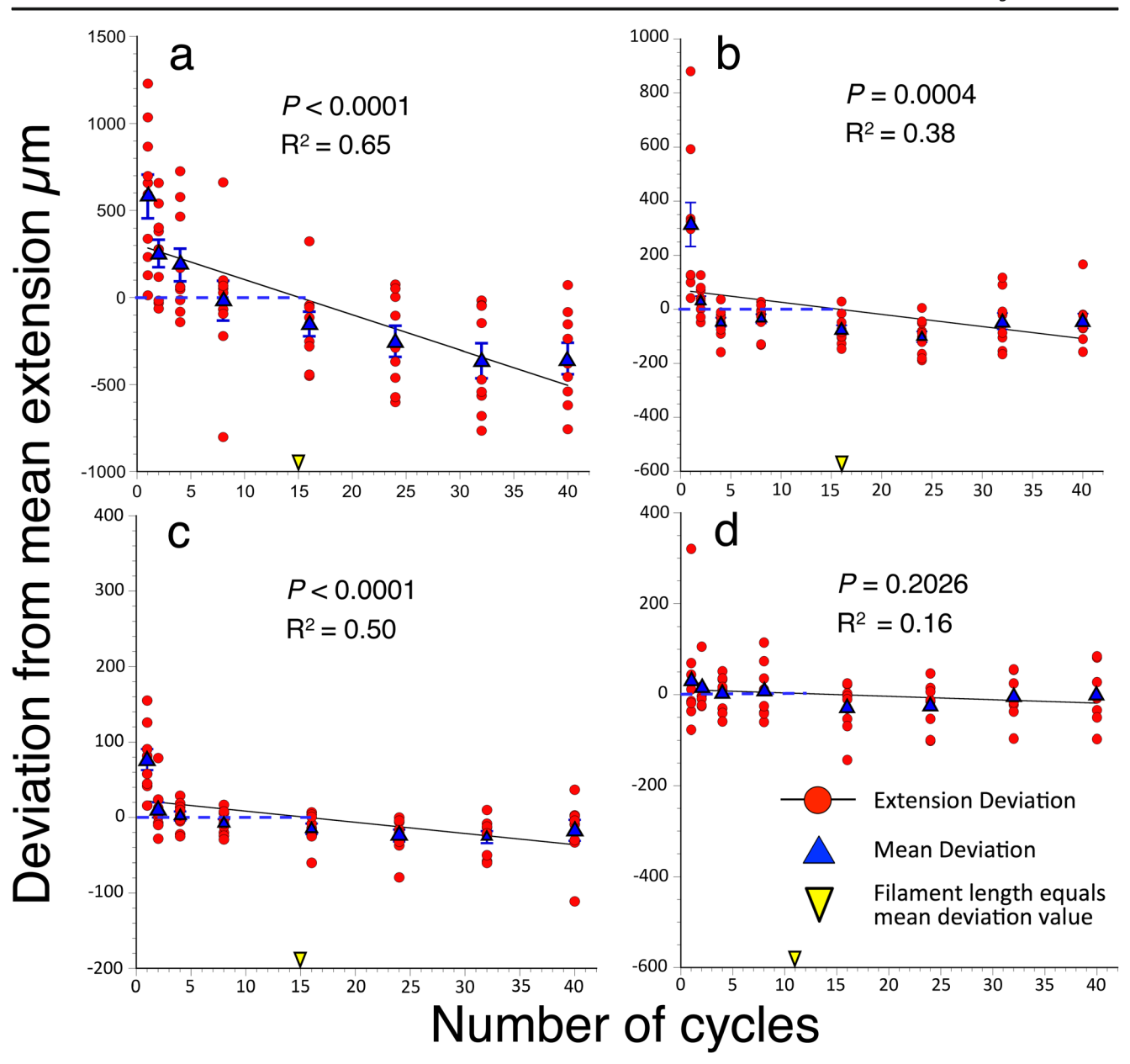


Fig. 5 Filament lengths at focal extensions at low humidity expressed as deviations from mean extension length. Neoscona crucifera (d) is the only species at this humidity where this relationship is not negative

contribute to both droplet hygroscopicity and glycoprotein plasticity. Although it is not possible to rule out evaporative water loss from droplets during cycling, this loss of LMMCs is a compelling explanation of our findings that is consistent with a developing understanding of the key role that LMMCs play in droplet performance (Townley and Tillinghast 2013; Amarpuri et al. 2015a, b; Singla et al. 2018). A contributing factor may have been that repeated droplet—probe contact compressed the glycoprotein, compacting its molecules and causing it to stiffen.

A surprising observation was how securely a droplet's glycoprotein core remained attached to the flagelliform axial fibers through cycling. In only four out of forty-four treatments did this anchor fail and droplets remain attached to the probe tip. In all cases of droplet detachment, when the naked flagelliform fibers were brought into contact with the droplet, which adhered to the probe, the droplet extended and at pull-off again remained attached to the probe. These observations are consistent with the presence of an anchoring granule at the center of a droplet that firmly, but not permanently, secures the glycoprotein mass to the flagelliform fibers (Opell and Hendricks 2010). In preparing focal droplets, we were able to slide adjacent droplets with no noticeable effect other than these droplets merging to form a larger droplet. Reattachment of droplets to flagelliform fibers suggests that a droplet's granule may represent a configurational change in glycoprotein as



10 Page 12 of 15 Sci Nat (2019) 106: 10

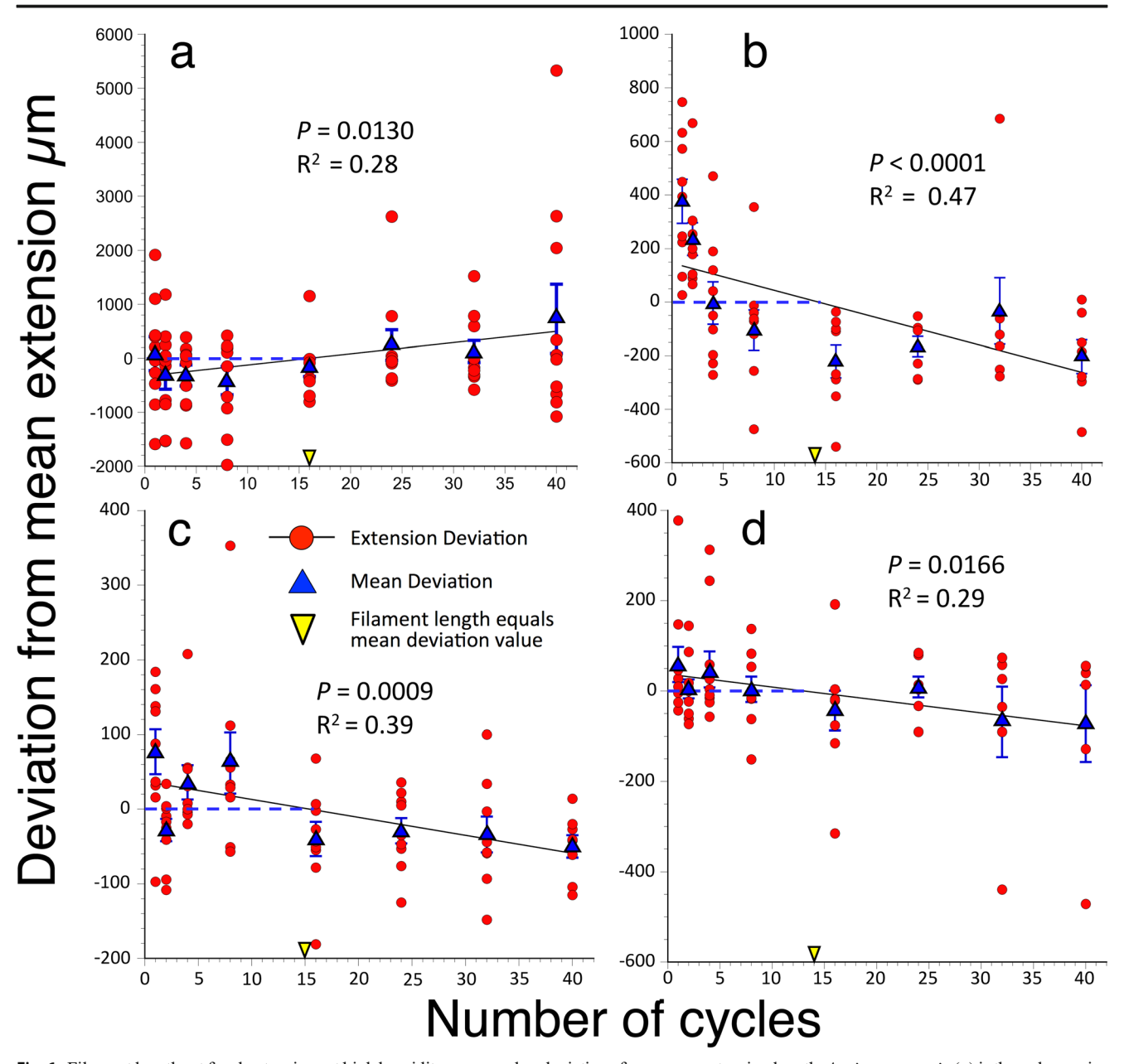


Fig. 6 Filament lengths at focal extensions at high humidity expressed as deviations from mean extension length. Argiope aurantia (a) is the only species at this humidity where this relationship is not negative

it interacts with flagelliform fiber binding sites and not another protein component in a droplet's glycoprotein core.

What do the results mean for natural capture thread function?

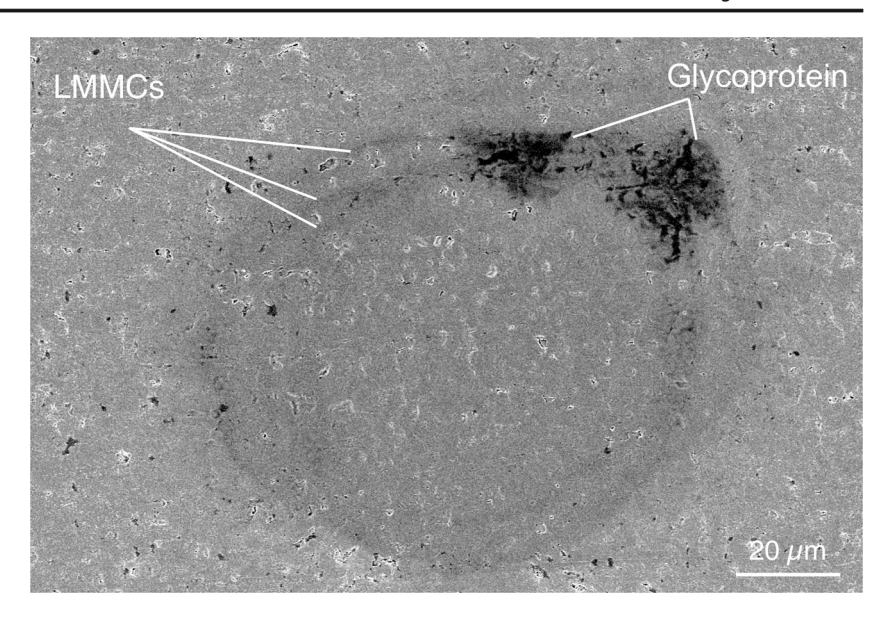
Our study characterized cycling of single droplets on a smooth surface. In nature, insects contact multiple droplets with surfaces of different textures. Surface texture is known to affect viscous thread adhesion (Opell and Schwend 2007). However, it is likely that our findings would apply at these higher levels, although it is unlikely that droplets would naturally experience

the extensive cycling we employed. The ability of viscous droplets to cycle is useful for orb weavers because it allows droplets to function after initial pull-off, when a struggling insect re-contacts a droplet. In the context of the suspension bridge system, the outer droplets of an adhering thread span contribute the most adhesive force and are typically the first to pull off (Opell and Hendricks 2009). Consequently, if these outer droplets can reattach, the suspension bridge would be reestablished. Although droplet filament length and volume decrease with repeated use, the limited changes in force and estimated work after a single extension would not substantially decrease prey retention. For subsequent insects, cycling



Sci Nat (2019) 106: 10 Page 13 of 15 10

Fig. 7 A scanning electron micrograph showing putative LMMCs and glycoprotein residues left on a steel surface after 40 extension cycles of a *L. cornutus* droplet



may not be relevant. When insects are trapped in an orb web, they either escape or are subdued by the spider, both of which result in significant damage to the capture threads. This structural damage may reduce cycling's usefulness in subsequent insect capture.

Conclusion

Viscoelastic orb weaver droplets are able to repeatedly adhere, extend, and pull off from a surface. This cycling, combined with their environmental response to humidity, classifies orb weaver droplets as smart materials. The capture thread has already been shown to function as a liquid-solid hybrid material when extended and compressed, and this study further documents the unique material properties of capture spiral silk (Elettro et al. 2015; Elettro et al. 2016). Extension cycling comes at a cost of reduced filament length, increased glycoprotein cohesion, and reduced aqueous layer volume, but a droplet's glycoprotein contact area, force at pull-off, and estimated work of extension remain unchanged after extensive reuse. It has been well documented that droplets absorb atmospheric humidity, with volume, filament length, and glycoprotein thickness changing significantly with changing relative humidity (Opell et al. 2018a, b). However, relative humidity does not appear to change how droplets of most species respond to cycling. Cycling allows for the spider to rely on its capture droplets after initial pull-off, increasing spider capture efficiency. The reusability of these droplets is remarkable because it requires all internal components of the droplet to continue their elaborate interactions, many of which we do not fully understand. This durability is also an important characteristic for glycoprotein mimicking adhesives. Not only are orb weaver droplets self-assembled aqueous glues made in ambient conditions (instead of factories), but these adhesives are also reusable, indicating that glycoprotein mimicking adhesives could be significantly more eco-friendly than existing industry adhesives.

Acknowledgments We would like to acknowledge Stephen McCartney for his assisted use of the LEO FESEM at Virginia Tech's Nanoscale Characterization and Fabrication Laboratory.

Funding support We would like to acknowledge the National Science Foundation for funding this study (grant IOS-1257719).

Compliance with ethical standards

Competing interests The authors declare that they have no competing interests in this study.

Publisher's note Springer Nature remains neutral with regard to jurisdictional claims in published maps and institutional affiliations.

References

Adams MR (2000) Choosing hunting sites: web site preferences of the orb weaver spider, *Neoscona crucifera*, relative to light cues. J Insect Behav 13(3):299–305

Amarpuri G, Chaurasia V, Jain D, Blackledge TA, Dhinojwala A (2015a) Ubiquitous distribution of salts and proteins in spider glue enhances spider silk adhesion. Sci Rep 5(9053): 1–7. https://doi.org/10.1038/ srep09030

Amarpuri G, Zhang C et al (2015b) Spiders tune glue viscocity to maximize adhesion. Am Chem Soc 9(11):11472–11478. https://doi.org/10.1021/acsnano.5b05658

Ayoub NA, Garb JE, Tinghitella RM, Collin MA, Hayashi CY (2007) Blueprint for a high-performance biomaterial: full-length spider dragline silk genes. PLoS One 2(6):e514. https://doi.org/10.1371/journal.pone.0000514

Blackledge TA, Eliason CM (2007) Functionally independent components of prey capture are architecturally constrained in spider orb



- webs. Biol Lett 3(5):456–458. https://doi.org/10.1098/rsbl.2007.
- Blackledge TA, Hayashi CY (2006) Silken toolkits: biomechanics of silk fibers spun by the orb web spider Argiope argentata (Fabricius 1775). J Exp Biol 209:2452–2461. https://doi.org/10.1242/jeb. 02275
- Blackledge TA, Scharff N, Coddington JA, Szuts T, Wenzel JW, Hayashi CY, Agnarsson I (2009) Reconstructing web evolution and spider diversification in the molecular era. PNAS 106(13):5229–5234 https://www.pnas.orgcgidoi10.1073pnas.0901377106
- Bond JE, Opell BD (1998) Testing adaptive radiation and key innovation hypothesis in spiders. Evolution 52(2):403–414
- Bradley RA (2013) Common spiders of North America. University of Califronia Press, Berkeley
- Carrel JE (2008) The effect of season of fire on density of female garden orbweavers (Araneae: Araneidae: Argiope) in Florida scrub. Fla Entomol 91(2):332–334
- Choresh O, Bayarmagnai B, Lewis RV (2009) Spider web glue: two proteins expressed from opposite strands of the same DNA sequence. Biomacromolecules 10(10):2852–2856. https://doi.org/10.1021/bm900681w
- Coddington JA (1989) Spinneret silk spigot morphology: evidence for the monophyly of orbweaving spiders, Cyrtophorinae (Araneidae), and Group Theridiidae plus Nesticidae. J Arachnol 17:71–95
- Collin MA, Clarke TH, Ayoub NA, Hayashi CY (2016) Evidence from multiple species that spider silk silk glue component ASG2 is a spidroin. Sci Rep 6. https://doi.org/10.1038/srep21589
- Concha A, Mellado P, Morera-Brenes B, Sampaio Costa C, Mahadevan L, Monge-Nájera J (2015) Oscillation of the velvet worm slime jet by passive hydrodynamic instability. Nat Commun 6(6292). https://doi.org/10.1038/ncomms7292
- Dickinson GH, Vega IE, Wahl KJ, Orihuela B, Beyley V, Rodriguez EN, Everett RK, Bonaventura J, Rittschof D (2009) Barnacle cement: a polymerization model based on evolutionary concepts. J Exp Biol 212:3499–3510
- Edmonds DT, Vollrath F (1992) The contribution of atmospheric water vapour to the formation and efficiency of a spider's capture web. R Soc 248:145–148. https://doi.org/10.1098/rspb.1992.0055
- Elbaum R, Zaltzman L, Burgert I, Fratzl P (2007) The role of wheat awns in the seed dispersal unit. Science 316:884–886. https://doi.org/10.1126/science.1140097
- Elettro H, Neukirch S et al (2016) In-drop capillary spooling of spider capture thread inspires hybrid fibers with mixed solid–liquid mechanical properties. PNAS 113(22):6143–6147
- Elettro H, Vollrath F, Antkowiak A, Neukirch S (2015) Coiling of an elastic beam inside a disk: a model for spider-capture silk. Int J Non Linear Mech 75:59–66
- Enders F (1977) Web-site selection by orb-web spiders, particularly Argiope aurantia (Lucas). Anim Behav 25(3):694–712
- Foelix RF (2011) Biology of Spiders, 3rd Edition. Oxford University Press. New York
- Gaddy L (1987) Orb-weaver abundance in three forested communities in the Southern Appalacian Mountains of South Carolina. J Arachnol 15:273–275
- Garb JE, Ayoub NA, Hayashi CY (2010) Untangling spider silk evolution with spidroin terminal domains. BMC Evol Biol 10(243):243. https://doi.org/10.1186/1471-2148-10-243
- Gatesy J, Hayashi C, Motriuk D, Woods J, Lewis R (2001) Extreme diversity, conservation, and convergence of spider silk fibroin sequences. Science 291(5513):2603–2605. https://doi.org/10.1126/ science.1057561
- Hebda DA, White SR (1995) Effect of training conditions and extended thermal cycling on nitinol two-way shape memory behavior. Smart Mater Struct 4:298–304
- Hoogenboom R (2014) Temperature-responsive polymers: properties, synthesis and applications. In: Aguilar MR, Román JS (eds) Smart

- polymers and their applications. Woodhead Publishing, Cambridge, pp 15-44
- Huang Y, Wang Y, Sun L, Agrawal R, Zhang M (2015) Sundew adhesive: a naturally occurring hydrogel. J R Soc Interface 12(107):20150226. https://doi.org/10.1098/rsif.2015.0226
- Jain D, Sahni V, Dhinojwala A (2014) Synthetic adhesive attachment discs inspired by spider's pyriform silk architecture. J Polym Sci B Polym Phys 52:553–560. https://doi.org/10.1002/polb.23453
- Jensen RA, Morse DE (1988) The bioadhesive of *Phragmatopoma* californica tubes: a silk-like cement containing L-DOPA. J Comp Physiol B 158(3):317–324. https://doi.org/10.1007/BF00695330
- Kamila S (2013) Introduction, classification and applications of smart materials: an overview. Am J Appl Sci 10(8):876–880. https://doi. org/10.3844/ajassp.2013.876.880
- Kamino K (2010) Molecular design of barnacle cement in comparison with those of mussel and tubeworm. J Adhes 86:96–110
- Li D, Huson MG, Graham LD (2008) Proteinaceous adhesive secretions from insects, and in particular the egg attachment glue of Opodiphthera sp. moths. Arch Insect Biochem Physiol 69(2):85–105. https://doi.org/10.1002/arch.20267
- Liao C-P, Blamires SJ, Hendricks ML, Opell BD (2015) A re-evaluation of the formula to estimate the volume of orb web glue droplets. J Arachnol 43:97–100
- Mackay RJ, Wiggins GB (1979) Ecological diversity in Trichoptera. Annu Rev Entomol 24:185–208
- Mead-Hunter R, King AJC, Mullins BJ (2012) Plateau Rayleigh instability simulation. Langmuir 28:6731–6735
- Naldrett MJ (1993) The importance of sulphur cross-links and hydrophobic interactions in the polymerization of barnacle cement. J Mar Biol Assoc India 73:689–702
- Opell BD, Clouse ME, Andrews SF (2018a) Elastic modulus and toughness of orb spider glycoprotein glue. PLoS One 13(5):e0196972. https://doi.org/10.1371/journal.pone.0196972
- Opell BD, Hendricks ML (2007) Adhesive recruitment by the viscous capture threads of araneoid orb-weaving spiders. J Exp Biol 210: 553–560. https://doi.org/10.1242/jeb.02682
- Opell BD, Hendricks ML (2009) The adhesive delivery system of viscous capture threads spun by orb-weaving spiders. J Exp Biol 212:3026–3034. https://doi.org/10.1242/jeb.030064
- Opell BD, Hendricks ML (2010) The role of granules within viscous capture threads of orb-weaving spiders. J Exp Biol 213:339–346. https://doi.org/10.1242/jeb.036947
- Opell BD, Jain D, Dhinojwala A, Blackledge TA (2018b) Tuning orb spider glycoprotein glue performance to habitat humidity. J Exp Biol 221:jeb161539. https://doi.org/10.1242/jeb.161539
- Opell BD, Karinshak SE, Sigler MA (2013) Environmental response and adaptation of glycoprotein glue within the droplets of viscous prey capture threads from araneoid spider orb-webs. J Exp Biol 216: 3023–3034. https://doi.org/10.1242/jeb.084822
- Opell BD, Schwend HS (2007) The effect of insect surface features on the adhesion of viscous capture threads spun by orb-weaving spiders. J Exp Biol 210:2352–2360
- Opell BD, Sigler S (2011) Humidity affects the extensibility of an orbweaving spider's viscous thread droplets. J Exp Biol 214:2988– 2993. https://doi.org/10.1242/jeb.055996
- Palacio MLB, Bhushan B (2012) Bioadhesion: a review of concepts and applications. R Soc 370(1967):2321–2347. https://doi.org/10.1098/ rsta.2011.0483
- Sahni V, Blackledge TA, Dhinojwala A (2010) Viscoelastic solids explain spider web stickiness. Nat Commun 1(19):1–4. https://doi.org/10.1038/ncomms1019
- Sahni V, Blackledge TA, Dhinojwala A (2011) Changes in the adhesive properties of spider aggregate glue during the evolution of cobwebs. Sci Rep 1(41):1–8. https://doi.org/10.1038/srep00041
- Sahni V, Miyoshi T, Chen K, Jain D, Blamires SJ, Blackledge TA, Dhinojwala A (2014) Direct solvation of glycoproteins by salts in



Sci Nat (2019) 106: 10 Page 15 of 15 **10**

spider silk glues enhances adhesion and helps to explain the evolution of modern spider orb webs. Biomacromolecules 15:1225–1232. https://doi.org/10.1021/bm401800y

- SAS Intitute Inc. C, NC (1989-2007). JMP pro, 13
- Sensenig AT, Agnarsson I et al (2010) Behavioral and biomaterial coevolution in spider orb webs. J Evol Biol 23:1839–1856. https://doi.org/10.1111/j.1420-9101.2010.02048.x
- Sensenig AT, Kelly SP, Lorentz KA, Lesher B, Blackledge TA (2013) Mechanical performance of spider orb webs is tuned for high-speed prey. J Exp Biol 216:3388–3394. https://doi.org/10.1242/jeb. 085571
- Sensenig AT, Lorentz KA, Kelly SP, Blackledge TA (2012) Spider orb webs rely on radial threads to absorb prey kinetic energy. J R Soc Interface 9(73):1880–1892
- Singla S, Amarpuri G, Dhopatkar N, Blackledge TA, Dhinojwala A (2018) Hygroscopic compounds in spider aggregate glue remove interfacial water to maintain adhesion in humid conditions. Nat Commun 9:1890. https://doi.org/10.1038/s41467-018-04263-z
- Smith RC (2006) Smart Material Systems. Chapter 1.1. Society for Industrial and Applied Mathematics, Philadelphia, pp 1–5
- Talbot D (2003) Smart materials. In: MaMSAS (ed) Institute of materials, pp 1-17

- Tillinghast EK, Townley MA et al (1993) The adhesive glycoprotein of the orb of *Argiope aurantia* (Araneae, Araneidae). Mater Res Soc Symp Proc 259:154–165
- Townley MA, Bernstein DT, Gallagher KS, Tillinghast EK (1991) Comparative study of orb web hygroscopicity and adhesive spiral composition in three araneid spiders. J Exp Zool 259(2):154–165. https://doi.org/10.1002/jez.1402590203
- Townley MA, Tillinghast EK (2013) Aggregate silk gland secretions of araneoid spiders. Springer-Verlag, Berlin Heidelberg
- Vollrath F, Edmonds DT (1989) Modulation of the mechanical properties of spider silk by coating with water. Nature 340:305–307. https:// doi.org/10.1038/340305a0
- Vollrath F, Tillinghast EK (1991) Glycoprotein glue beneath a spider web's aqueous coat. Naturwissenschaften 78(12):557–559. https:// doi.org/10.1007/BF01134447
- Waite HJ (2017) Mussel adhesion—essential footwork. J Exp Biol 220: 517–530
- Wolff JO, Grawe I, Wirth M, Karstedt A, Gorb SN (2015) Spider's superglue: thread anchors are composite adhesives with synergistic hierarchical organization. Soft Matter 11(12):2394–2403. https://doi. org/10.1039/c4sm02130d

